ISSN 1061-8309, Russian Journal of Nondestructive Testing, 2023, Vol. 59, No. 10, pp. 1052–1060. © Pleiades Publishing, Ltd., 2023.
Russian Text © The Author(s), 2023, published in Defektoskopiya, 2023, No. 10, pp. 43–52.

X-RAY METHODS

Soft X-ray Based Quality Control Technique for Structural Elements Made of Lightweight Materials

I. A. Kishin[a,b,*], E. Y. Kidanova[a,], A. S. Kubankin[a,b,***], and V. S. Sotnikova[c,****]**

[a] *Belgorod State National Research University, Belgorod, 308015 Russia*

[b] *Lebedev Physical Institute of the Russian Academy of Sciences (FIAN), Moscow, 119991 Russia*

[c] *Belgorod State Technological University named after V.G. Shukhov, Belgorod, 308012 Russia*

**e-mail: ivan.kishin@mail.ru*

***e-mail: 28kidanova28@gmail.com*

****e-mail: askubankin@gmail.com*

*****e-mail: levultra@gmail.com*

Received June 14, 2023; revised September 1, 2023; accepted September 4, 2023

Abstract—The paper describes a nondestructive testing method for the study of structural elements made of lightweight materials. The method is based on the analysis of soft X-ray spectra. The test results for a pipe made of carbon fiber with an average wall thickness of 1 mm are presented. The possibility of constructing maps of the distribution of pipe wall thickness with an accuracy above 10 μm is shown.

Keywords: X-ray testing, soft X-ray radiation, semiconductor detector, thickness gauging, nondestructive testing method

DOI: 10.1134/S1061830923700559

INTRODUCTION

The testing of the strength and mass-dimensional characteristics of structural elements is a mandatory procedure for the development of plant parts. Currently, the following methods of nondestructive quality control of structures are widely used [1–12]: acoustic emission, acoustic, X-ray, thermography, hydraulic testing, shearography, etc. The choice of the flaw detection method depends on the properties of the test object and the required result accuracy.

At the moment, the most common method of quality control of pipelines made of lightweight composite materials is the acoustic-emission flaw detection method, based on detecting and analyzing acoustic waves generated by defects inside the sample.

Of all the available flaw detection methods, X-ray flaw detection deserves special attention [10, 11], which, along with the acoustic emission method [12], can be used directly in the production process of the examined structures. However, unlike the acoustic emission method, X-ray flaw detection allows detecting defects both on the surface and inside the material. The advantage of X-ray flaw detection is its applicability to a wide range of materials, including metals, plastics, and various types of composites. X-ray testing is practically independent of external factors such as humidity, temperature, and lighting.

In most cases, X-ray flaw detection is used to check the integrity and suitability of metal structures, for example, pipeline welds [13]. At the same time, the development of new ways to implement the method of X-ray flaw detection for pipelines made of lightweight composite materials remains an urgent task.

In this paper, a new technique of nondestructive X-ray inspection is described and an experimental stand for the study of structural elements made of lightweight materials is developed. The technique is based on the analysis of characteristic peaks in the soft X-ray radiation spectrum. The unit operates in the energy range from 1 to 10 keV in the mode of energy dispersion analysis of an X-ray signal transmitted through the test object and scattered by it. Tests performed on a carbon fiber pipe with a diameter of 48.4 mm and with an average wall thickness of 1 mm showed the possibility of constructing maps of the distribution of pipe wall thickness with an accuracy above 10 μm.

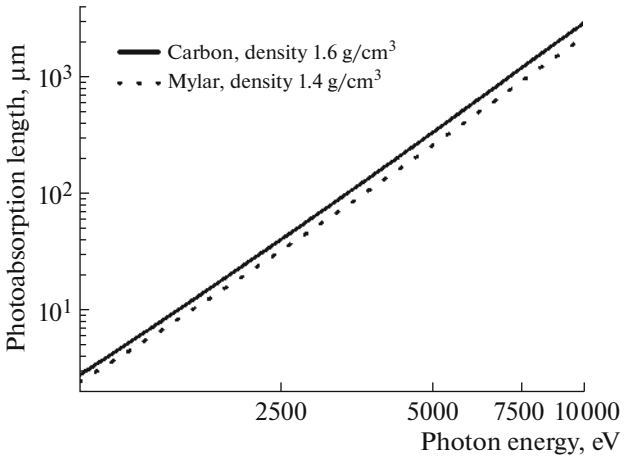

Fig. 1. Dependence of X-ray photoabsorption length: in carbon with density of 1.6 g/cm^3 (solid line), in Mylar with density 1.4 g/cm^3 (dotted line); the database [14] was used for calculation.

TECHNIQUE JUSTIFICATION

When X-rays pass through a layer of matter, the intensity of the radiation transmitted through the material decreases relative to the initial one due to scattering and absorption in this material. The following expression is used to determine the intensity of monochromatic radiation transmitted through the layer of the substance in question:

$$N = N_0 \times e^{-\mu \times L}, \tag{1}$$

where N_0 is the primary X-ray radiation intensity, L is the thickness of the absorbing layer of substance, and μ is the linear attenuation coefficient determined by the formula $\mu = 1/L_{abs}$, where L_{abs} is the photoabsorption length of monochromatic X-ray radiation.

If the initial X-ray flux and the flux after passing through the layer of the substance in question are known, the thickness of the attenuating layer L can be calculated using the following equation using expression (1) for a certain radiation energy:

$$L = -\ln\left(\frac{N}{N_0}\right) L_{abs}. \tag{2}$$

Expression (2) can be used to determine the thickness of the test object by selecting the energy of X-ray radiation in such a way as to ensure its partial absorption by the material.

In this work, we investigated a pipe made of carbon fiber with an outer diameter of 48.4 mm and an average wall thickness of 1 mm. To estimate the required spectral range, a model calculation was carried out, in which it was assumed that the pipe in question consists entirely of carbon with a density of 1.6 g/cm^3. Figure 1 shows the results of a model calculation of X-ray photoabsorption lengths in the spectral range 1–10 keV for carbon. The dotted line also indicates the dependence of the photoabsorption length on the radiation energy for a polyethylene terephthalate (Mylar) film with a density of 1.4 g/cm^3. It can be seen from the presented data that the photoabsorption lengths of Mylar and carbon are close in value, so we will consider them identical in this paper. Wrapping the pipe with a film made of Mylar (thickness 40 μm) made it possible to vary the thickness of the pipe wall and thereby evaluate the resolution of the proposed technique.

EXPERIMENTAL STAND

Given the specifics of this technique, in order to determine the thickness of the pipe wall, it is necessary that either a detector or an X-ray source be placed inside the pipe under study in the developed measurement scheme. Due to the fact that the described installation involves the diagnosis of pipes with a small diameter, it was decided to use a scheme in which the detector is placed inside the pipe (Fig. 2), which greatly facilitated the measurement process.

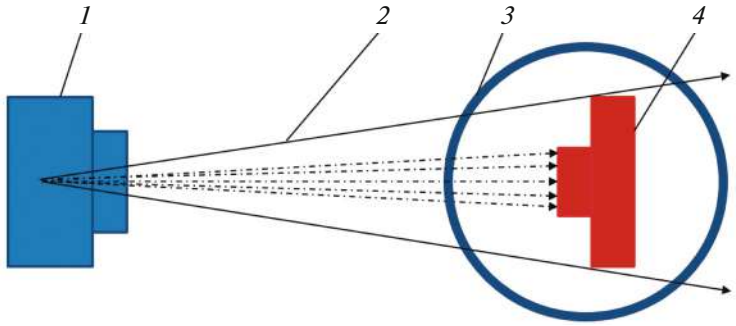

Fig. 2. Measurement scheme: (*1*) detector, (*2*) pipe, (*3*) X-rays, (*4*) X-ray tube.

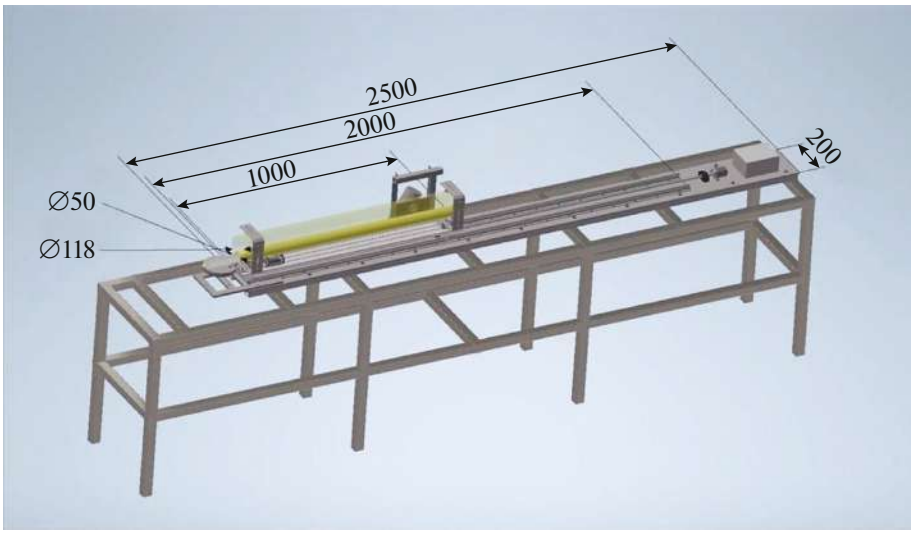

Fig. 3. Sketch of experimental stand.

The model of the manufactured stand is shown in Fig. 3. Rails with a length of 2 m are placed on a plate with a size of 2.5×0.2 m^2, along which a plate with a length of 1 m is moved using a motorized drive. The detector and the X-ray tube are fixed rigidly so that the output window of the X-ray tube is directed at the input window of the detector.

The measuring unit is shown in Fig. 4a. The diagnosed tube *1* is installed in the measurement position in such a way that detector *3* installed on mount *2* with collimator *4* is completely inside the tested pipe, to which X-ray radiation *5* from X-ray tube *6* is directed. The axisymmetric rotation of the pipe is carried out by special roller holder *7* and motorized roller *8*; the fasteners allow installing pipes with a diameter from 45 to 118 mm.

The motorized drives are controlled using a power driver installed on the plate, controlled by the operator based on the selected measurement mode using dedicated software written specifically for the described installation [15]. The created program in the scanning mode implements the rotation and linear movement of the pipe, while the detecting system remains stationary. The software allows one to set the scan area, time, and step of one measurement. The software is also used to control the X-ray detector.

In the described experimental stand, we used an X-123 FastSDD X-ray spectrometer (Amptek) in OEM configuration [16], consisting of a FastSDD semiconductor drift detector with a 12.5 μm beryllium window, a PA210 preamplifier, and a DP5 control board. The selected semiconductor detector has a high counting rate of more than 1 000 000 cps while maintaining high resolution. It can be noted that the detector proved itself well earlier and was used in experimental studies of X-ray radiation on accelerator complexes of relativistic [17] and ultrarelativistic electrons [18]. During the tests, the signal generation time was 0.8 μs; this ensured the photon recording efficiency of more than 95% in the spectral region of

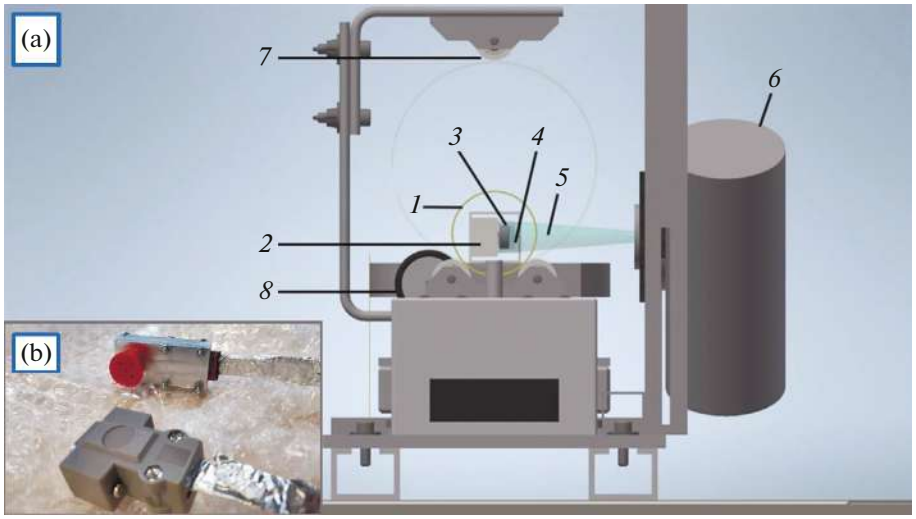

Fig. 4. Measuring unit (a): (*1*) diagnosed pipe, (*2*) detector holder, (*3*) X-ray spectrometer, (*4*) lead collimator, (*5*) X-ray radiation area, (*6*) X-ray tube, (*7*) roller holder, (*8*) rotary drive; detector used (b).

the K_α-chromium lines. Additionally, a lead collimator with an aperture of 1 mm was installed on the spectrometer.

The housing for the detector and preamplifier was made in such a way that the detector input window was directed to the output window of the X-ray tube, without interfering with the movement of the tube. This resulted in a compact detector configuration, characterized by small dimensions of $65 \times 25 \times 25$ mm^3 and preserving spectrometric characteristics (Fig. 4b). The created housing allows one to carry out research of pipes with a diameter from 45 to 118 mm.

Based on the results demonstrated in Fig. 1, and taking into account the fact that the wall thickness of the pipe under study can be quite large while the measurement time should be minimal, the best option was to use an X-ray tube with a chromium anode, in which the characteristic X-ray (CXR) energy of the K_α-line corresponds to the value of 5.41 keV. According to the simulation, the value of the photoabsorption length in carbon for this energy is 430 μm. An X-ray tube of Oxford Instruments 5000 series with a chromium anode [19] was used as an X-ray radiation source. The main characteristics of the tube are listed in Table 1. During the experiment, the following X-ray tube settings were used: accelerating voltage 9 kV, emission current 20 μA. The distance from the X-ray tube to the X-ray spectrometer was 130 mm.

EXPERIMENTAL TESTS OF THE STAND

Determining photoabsorption length in material. The tests were carried out on a section of carbon fiber pipe with an outer diameter of 48.4 mm and an average wall thickness of 1 mm. Since the exact elemental composition and density of the pipe material were unknown, the following approximations were used at the first stage of testing: the elemental composition of the pipe is unchanged throughout the volume and

Table 1. Characteristics of Oxford Instruments 5000 Series X-ray tube

Characteristics	Values
High voltage range	From 5 to 50 kV
Maximum power	50 W
Maximum beam current	1.0 mA
Focal spot size	200 μm
Window material and thickness	Be, 127 μm
Dimensions	180 mm D × ∅70 mm
Anode	Chromium

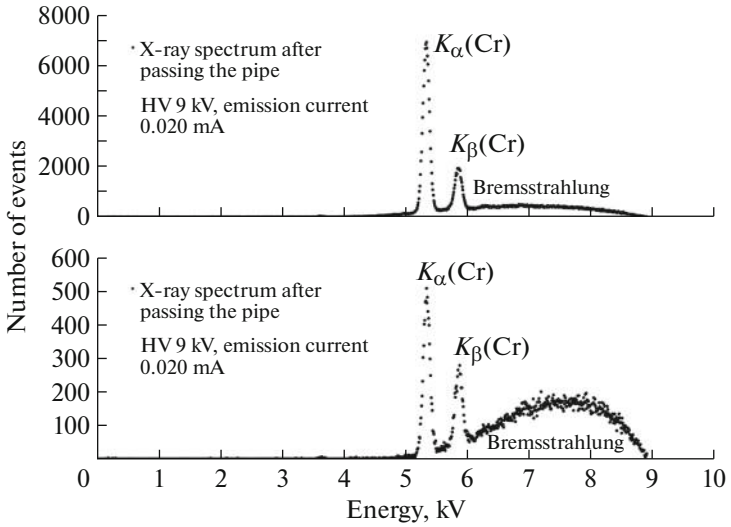

Fig. 5. X-ray spectra: X-ray tube spectrum (top); spectrum of radiation transmitted through pipe wall (bottom).

the initial wall thickness is 1 mm. These approximations can be used to estimate the deviation of the pipe wall thickness based on the developed approach.

One of the characteristics of the problem under consideration is the photoabsorption length in the pipe material. To determine this characteristic, measurements of X-ray spectra without a wall and radiation attenuated by one pipe wall were performed. The wall was placed between the X-ray tube and X-ray spectrometer, while all other measurement parameters were unchanged, namely: the geometry of the measurements, the dimensions of the collimator, and the settings of the X-ray tube.

Measurement of the X-ray tube spectrum with no wall, performed for 15 seconds, showed the integral number of photons 109 997 and 36 211 for the K_α- and K_β-lines of chromium, respectively. Similar measurements with attenuation of radiation by one pipe wall showed values of 8000 and 5625, respectively. Figure 5 shows the measured spectra. It is worth noting that the measurement results showed a high energy resolution of the 110 eV X-ray spectrometer in the energy range from 4 to 6 keV, which makes it possible to separate the contributions of the K_α- and K_β-chromium lines.

Using formula (2) and considering the fact that $L \approx 1$ mm (pipe wall thickness), we find the photoabsorption length $L_{abs} = 382$ μm for the photon energy of 5.41 keV and $L_{abs} = 537$ μm for 5.95 keV. Taking into account the obtained measurement results and using the approximation in which it is assumed that the pipe consists only of carbon, the density of the pipe material was determined using the database [14] as ~1.75 g/cm^3.

Determining wall thickness in carbon fiber pipe. In the first series of measurements of the pipe wall thickness, the detector was located at a distance of 15 mm from the pipe end. Measurements of the radiation spectrum transmitted through the pipe were performed in the scanning mode along a circle with a step along the outer surface of the tube of 1 mm (2.368°), the pipe rotated around its own axis with the X-ray tube and X-ray spectrometer unchanged. The geometry of the experiment made it possible to measure the average thickness of a cylindrical fragment of a pipe wall with a diameter of approximately 1 mm. Taking into account the fact that the circumference of the outer surface of the pipe is 152 mm, 152 measurements were necessary for a full scan. To verify the correctness of the obtained results, the number of measured points was increased by 7, which made it possible to compare the first and last 7 measurement points, which should be identical. Before starting the measurements, the position of the visually observed area of the pipe, in which there was presumably a longitudinal seam, was recorded. This area had the shape of a strip and was visually observed along the surface of the pipe from one or two sides, depending on the pipe section. The results of measurements of the total number of photons of K_α-chromium lines for each scanning point are shown in Fig. 6a.

From the presented results, the heterogeneity of the recorded signal is visible, while the maximum distribution is observed in the seam region, which indicates a reduced density of the substance, i.e., a decrease in the thickness of the pipe wall or the presence of some defects. One can also note a good repeatability

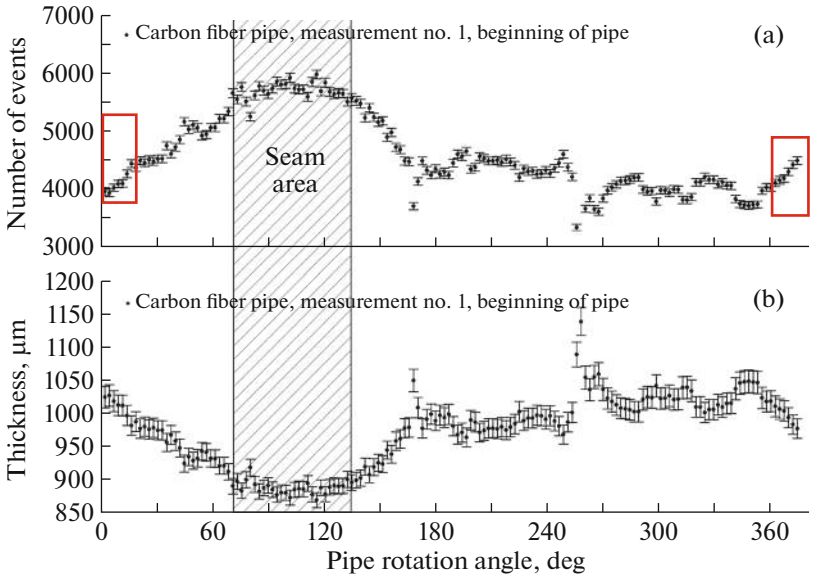

Fig. 6. Measurement series no. 1: (a) results of measurements of the total number of photons of K_α-chromium lines for each scanning point of carbon fiber pipe; (b) results of measurements of a carbon fiber pipe wall thickness made on the basis of absorption of K_α-chromium lines. The red rectangles are the measurement areas that overlap when the pipe rotates.

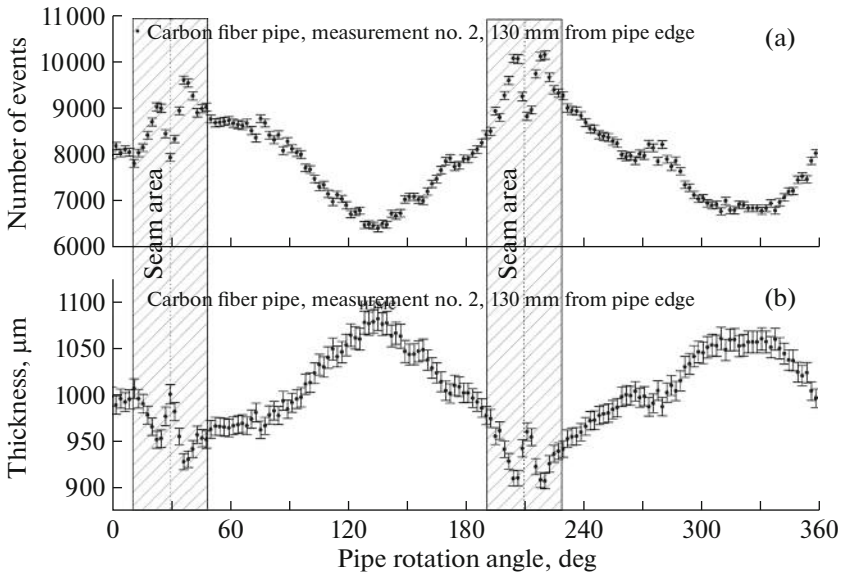

Fig. 7. Measurement series no. 2: (a) results of measurements of the total number of photons of K_α-chromium line for each scanning point of carbon fiber pipe; (b) results of measurements of carbon fiber pipe wall thickness made on the basis of absorption of the K_α-chromium lines.

of the results for overlapping areas (rectangles) in shape and signal strength. Recalculation of the measurement results into the wall thickness using formula (2) gives the results shown in Fig. 6b.

In the second series of measurements, the distance from the pipe edge to the detector was 130 mm. The measurements were carried out similarly to the first series of measurements, the obtained data of the total number of photons of K_α-chromium lines for each scanning point are shown in Fig. 7a. Figure 7b shows the result of conversion by formula (2) to the value of the pipe wall thickness. The measurement error was 10 μm. The presented dependences show a similar distribution of the substance concentration in the pipe wall with the results of the first series of the experiment, except for the occurrence of a second peak in the measured distribution. The distance between the two peaks was 180°.

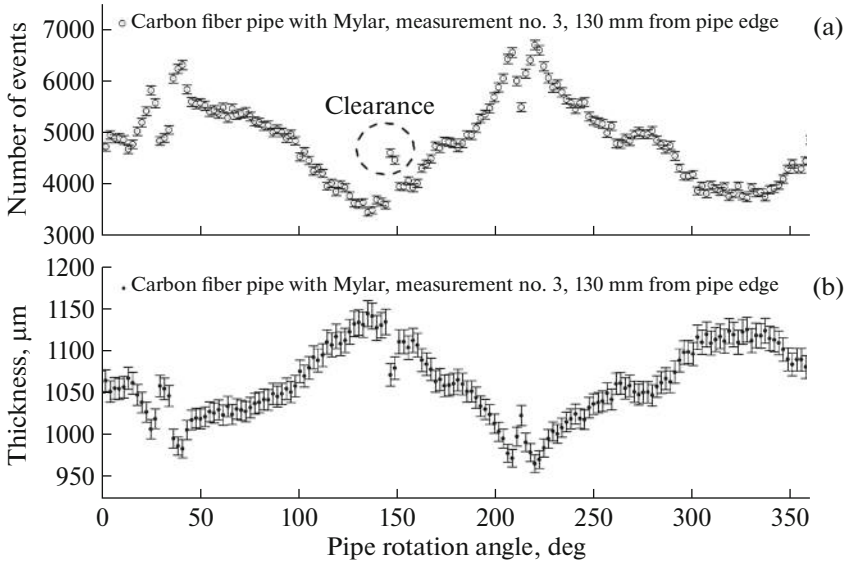

Fig. 8. Measurement series no. 3: (a) results of measurements of the total number of photons of K_α-chromium lines for each scanning point of carbon fiber pipe; (b) results of measurements of carbon fiber pipe wall thickness made on the basis of absorption of K_α-chromium lines.

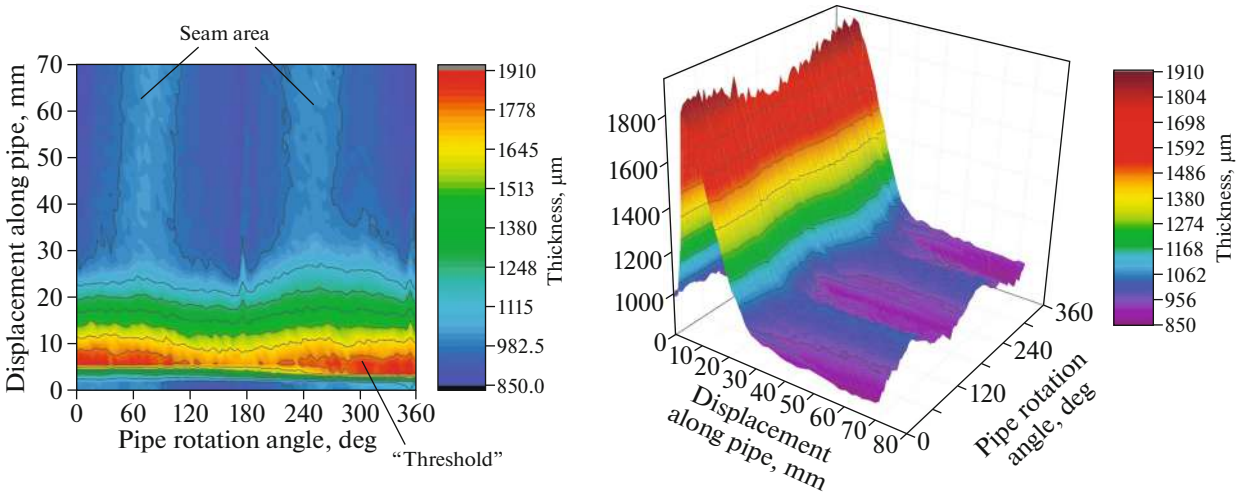

Fig. 9. Measurement series no. 4: automatic scanning of pipe section (longitudinal seams in light blue area, "threshold" in red area).

The task for the third series of measurements was to test the sensitivity of the proposed approach. The measurements used the settings identical to the second series of measurements. To accomplish this task, the outer surface of the pipe was wrapped with a single layer of Mylar film with a thickness of 60 μm, while a gap of approximately 2 mm was left between the closing edges. The measurement results are shown in Fig. 8a.

The pipe position for which the X-ray radiation interacted with the gap left at the junction of the edges of the Mylar film can be determined by increasing the number of events on the curve in Fig. 8a (indicated by an oval). It can be seen that the number of recorded photons increases sharply in this area: the graph clearly demonstrates that the difference between the peak and the base is about 5 statistical errors, a figure that is sufficient for reliable interpretation of the data obtained.

The result of calculating the pipe wall thickness by formula (2) with the assumption that photoabsorption in Mylar and the pipe is the same for a given energy is shown in Fig. 8b. The measured maximum wall thickness of the pipe wrapped with Mylar is 1.14 mm ±10 μm, and the minimum thickness

is 0.96 mm ± 10 μm. In the case where only the pipe was measured, the maximum thickness of the pipe was 1.08 mm ± 10 μm, and the minimum thickness was 0.90 mm ± 10 μm.

A section of pipe with a length of 70 mm was scanned under the same operating conditions of the experimental stand. The scan was performed automatically using the software described above. The resulting heat map is shown in Fig. 9. The image indicates pipe inhomogeneity, namely, the presence of two longitudinal seams and an axisymmetric "threshold" with a height of ~2 mm, the thickness of which was additionally measured with a caliper. In Fig. 9, the longitudinal seams correspond to the light blue area, and the "threshold" is red.

CONCLUSIONS

A new nondestructive testing technique has been developed [20] for studying structural elements made of lightweight materials. The approbation of the technique performed on the created experimental stand made it possible to measure the wall thickness of carbon fiber pipes with the required sensitivity. In particular, for a pipe with a length of 100 cm, an outer diameter of 48 mm, and an average wall thickness of 1 mm made of carbon fiber, the measurements show a variation in the thickness of the pipe wall within ±100 μm of the average thickness, disregarding the "threshold" of height 2 mm. Correlation of the reduced wall thickness areas and the location of "seams" of the pipe was established. It is shown that the sensitivity of measurements can reach an investigated pipe wall thickness resolution on the order of 10 μm with a spatial resolution of 0.78 mm^2 and a measurement time of thickness of one pipe area on the order of 10 s.

ACKNOWLEDGMENTS

The work was carried out using equipment based at the Center of High Technologies of Belgorod State Technological University named after V.G. Shukhov.

FUNDING

The work was supported by a program of the Ministry of Education and Science of the Russian Federation for higher education establishments (project no. FZWG-2020–0032 (2019–1569).

CONFLICT OF INTEREST

The authors of this work declare that they have no conflicts of interest.

REFERENCES

1. Gholizadeh, S., A review of non-destructive testing methods of composite materials, *Procedia Struct. Integrity,* 2016, vol. 1, pp. 50–57.
2. Jian Chen, Zhenyang Yu, and Haoran Jin, *Nondestructive testing and evaluation techniques of defects in fiber-reinforced polymer composites: A review*, *Sec. Polymeric Compos. Mater.,* 2022, vol. 9.
3. Naginaev, K.E. and Savel'ev, V.N., Acoustic emission control of a pipeline model under cyclic and static loading, *Izv. Vyssh. Uchebn. Zav.,* 2007, no. 6, pp. 54–57.
4. Danilov, V.N., Ushakov, V.M., and Rimkevich, A.I., Investigating the possibilities of assessing the state of the metal structure of pipelines in service by ultrasonic method, *Russ. J. Nondestr. Test.,* 2021, no. 8, pp. 635–646.
5. Knyazyuk, L.V. and Kruglova, E.V., Determination of welded joint flaw dimensions on the basis of scanned X-ray images, *Russ. J. Nondestr. Test.,* 2004, vol. 40, no. 1, pp. 57–60.
6. Fernandes, H., Hai Zhang, Figueiredo, A., Ibarra-Castanedo, C., Gilmar Guimarares, and Maldague, X., Carbon fiber composite inspection and defect characterization using active infrared thermography: Numerical simulations and experimental results, *Appl. Optics,* 2016, vol. 55, no. 34.
7. Vartanov, A.Z. and Nabatov, V.V., Thermographic control for construction (review article), *Gorn. Inf. Anal. Byull.,* 2011, no. 9, pp. 192–200.
8. Gulinin, D.A., Bitaeva, M.V., Gundorova, I.G., and Egovtseva, V.A., Features of hydraulic testing of pipelines in conditions of negative ambient temperatures, *Transp. Khranenie Nefteprod. Uglevodorodn. Syr'ya,* 2021, nos. 5–6, pp. 54–59.
9. Benedet, E., Fantin, V., Willeman, P., Junior, A., Schmitz, C., Cibra d'Almeida, F., Soares, S., Lana, D., and Perrut, V., The use of shearography technique to evaluate polymeric composite repairs—Case study, *Revista Materia,* 2017, vol. 22, no. 2.

10. Tarasov, S.Y., Rubtsov, V.E., Kolubaev, E.A., Gnyusov, S.F., and Kudinov, Y.A., Radioscopy of remnant joint line in a friction stir welded seam, *Russ. J. Nondestr. Test.,* 2015, vol. 51, no. 9, pp. 573–579.
11. Potrakhov, N.N., Zhamova, K.K., Bessonov, V.B., Gryaznov, A.Yu., and Obodovskii, A.V., Technology of operative X-ray control of products made of polymer composite materials, *Vestn. PNIPU,* 2015, no. 43, pp. 97–115.
12. Elizarov, S.V., Terent'ev, D.A., Medvedev, K.A., Ivanov, V.I., Khalimov, A.G., and Bardakov, V.V., Acoustic emission diagnostics of fiberglass pipes and fittings, *Kontrol' Diagn.,* 2021, vol. 24, no. 1, pp. 12–25.
13. Shleenkov, A.S., Novgorodov, D.V., and Konoval'chuk, V.O., *Investigation of defects in a longitudinal welded pipe seam*, *Fiz. Tekhnol. Innovats. VIII Mezhdunar. Molodezhn. Nauchn. Konf.* (Yekaterinburg, 2021), pp. 307–314.
14. Henke, B., Gullikson, E., and Davis, J., X-ray interactions: Photoabsorption, scattering, transmission, and reflection at $E = 50–30000$ eV, $Z = 1–92$, *At. Data Nucl. Data Tables,* 1993, vol. 54, no. 2, pp. 181–342.
15. Kischin, I.A., Kubankin, A.S., Kubankina, A.A., Nazhmudinov, R.M., Dronik, V.I., and Kozachenko, A.O., RF Patent no. 2022613325, 2022.
16. Amptek, OEM Solutions for XRF Systems. https://www.amptek.com/products/x-ray-detectors/oem-xrf-solutions/oem-solutions-for-xrf-systems. Accessed June 13, 2023.
17. Alekseev, V.I., Astapenko, V.A., Eliseev, A.N., Irribarra, E.F., Karpov, V.A., Kischin, I.A., Krotov, Yu.A., Kubankin, A.S., Nazhmudinov, R.M., Al-Omari, M., and Sakhno, S.V., Investigation of the mechanisms of generation of X-ray radiation in the interaction of relativistic electrons with matter at "Rentgen 1" installation, *Poverkhn. Rentgenovskie Sinkhrotronnye Neitr. Issled.,* 2017, no. 7, pp. 13–18.
18. Nazhmudinov, R.M., Shchagin, A.V., Kischin, I.A., Kubankin, A.S., Trofimenko, S.V., Potilitsin, A.P., Gogolev, A.S., Filatov, N.A., Kube, G., Potylitsina-Kube, N.A., Stanitzki, M., and Novokshonov, A., K-shell ionization cross section of Ti and Cu atoms by 1 and 2 GeV electrons, *J. Phys. B At. Mol. Optical Phys.,* 2021, vol. 54, no. 4, p. 045201.
19. Oxford Instruments. Jupiter 5000 Series Radiation Shielded X-ray Tube. https://xray.oxinst.com/x-ray-tube-products/x-ray-tube-assembly-radiation-shielded/jupiter-5000-series. Accessed June 13, 2023.
20. Kischin, I.A., Kubankin, A.S., Kubankina, A.A., and Firsov, D.G., A method for quality control of structural materials made from light elements, Know-How Certificate no. 426, 2022. Appl. June 2, 2022. Publ. June 29, 2022.